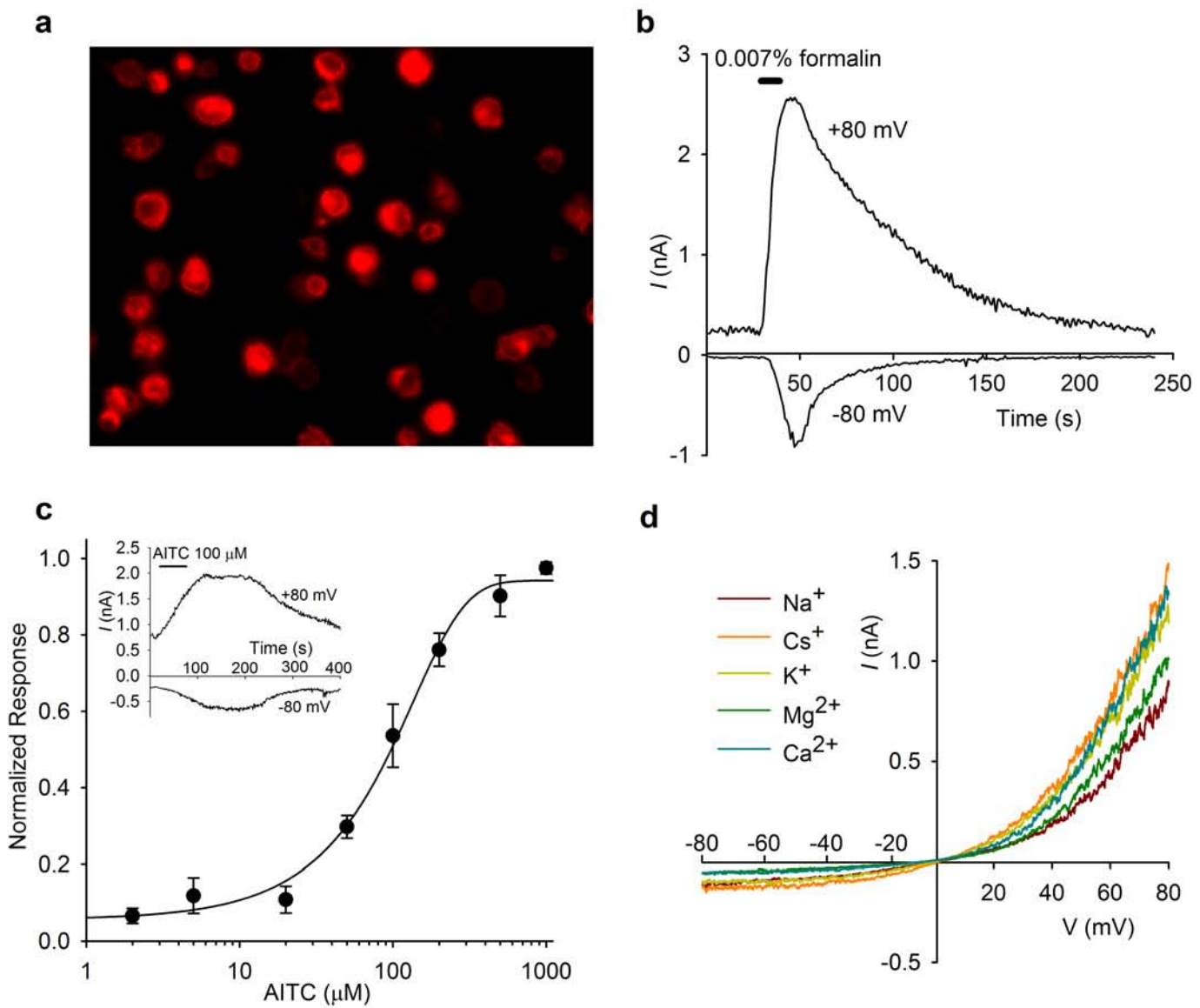
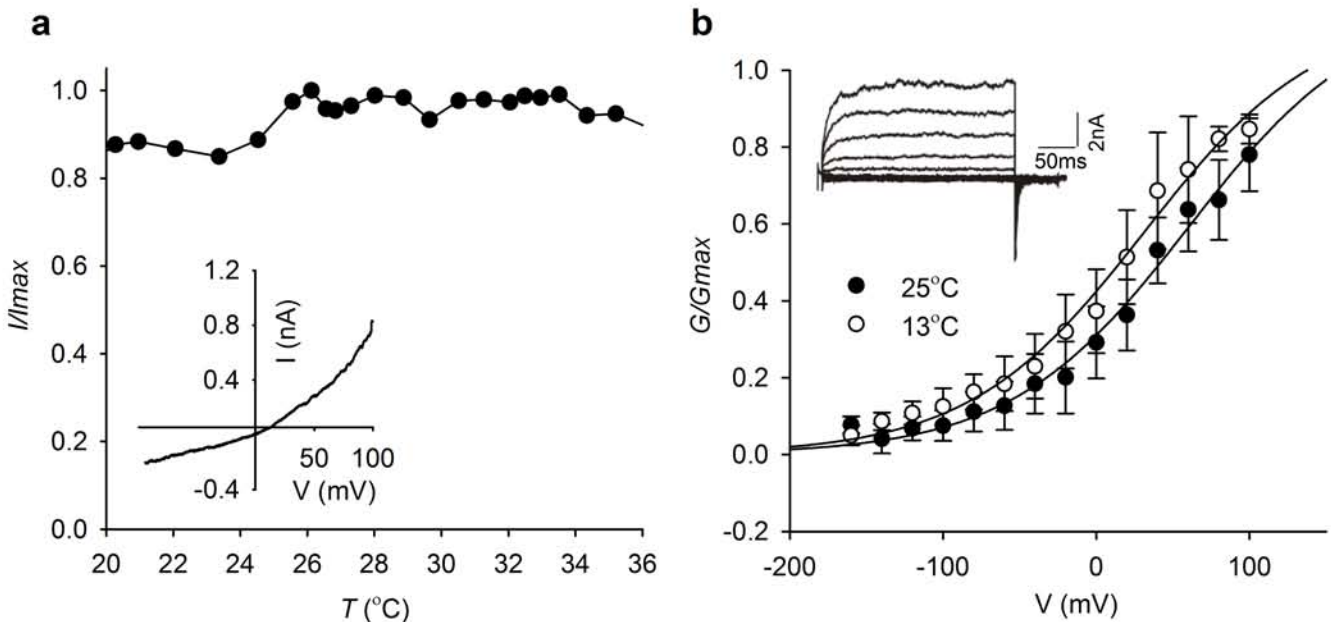


## Supplementary Figure 1. Robust expression of dTRPA1 in S2 cells



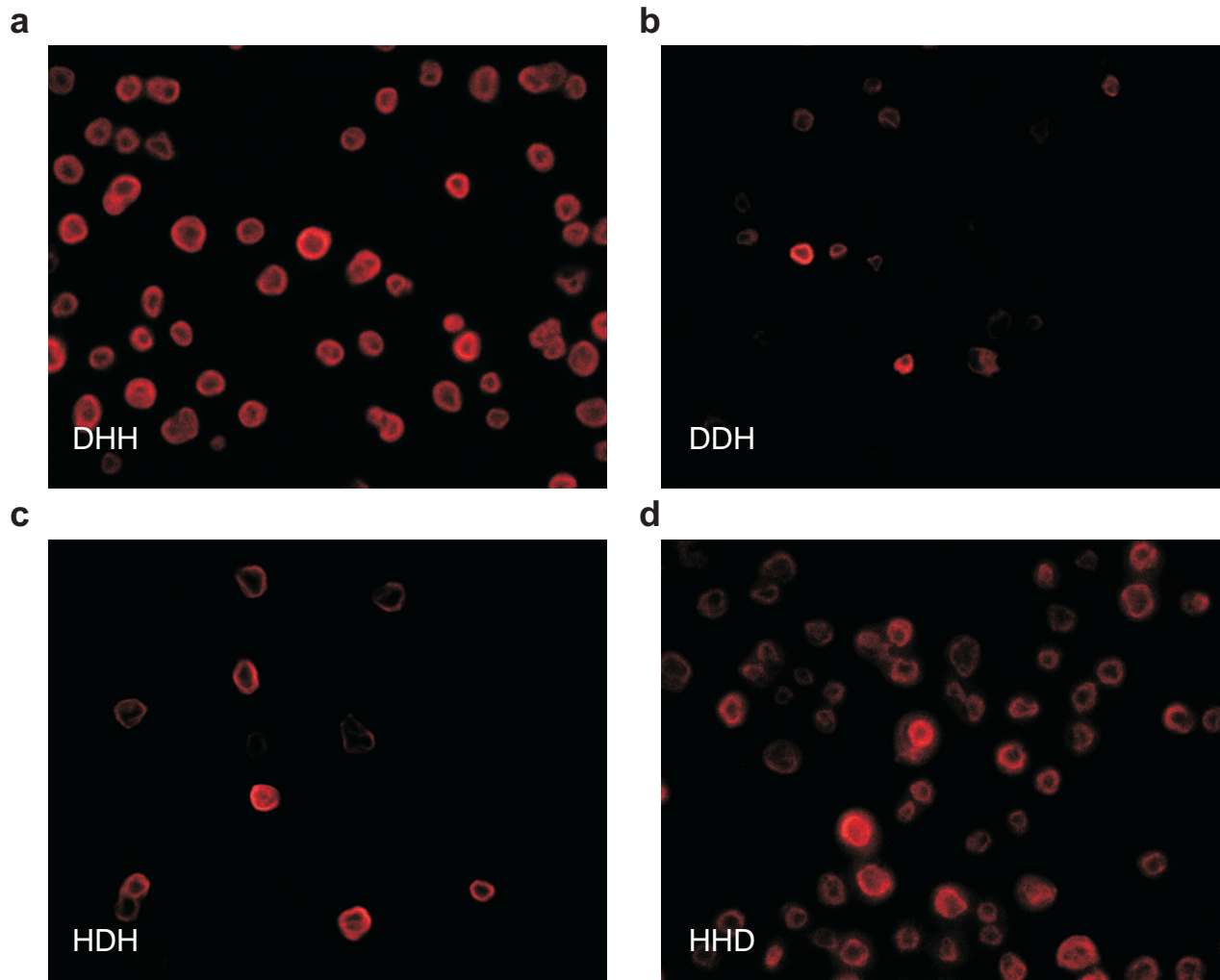
**Supplementary Figure 1.** Robust expression of dTRPA1 in *Drosophila* S2 cells. **(a)** Membrane expression of V5-epitope tagged dTRPA1. **(b)** dTRPA1 currents at +100 mV and -100 mV in S2 cells in response to a temperature ramp. **(c)** Concentration–response curve of maximum AITC evoked dTRPA1 currents measured at +80 mV, the EC<sub>50</sub> was  $99.7 \pm 7.2 \mu\text{M}$ . The inset shows a representative recording. **(d)** Current–voltage relationships for dTRPA1 in various extracellular solutions evoked by a voltage ramp from -80 mV to +80 mV over 400 ms.

## Supplementary Figure 2. Temperature sensitivity of hTRPA1



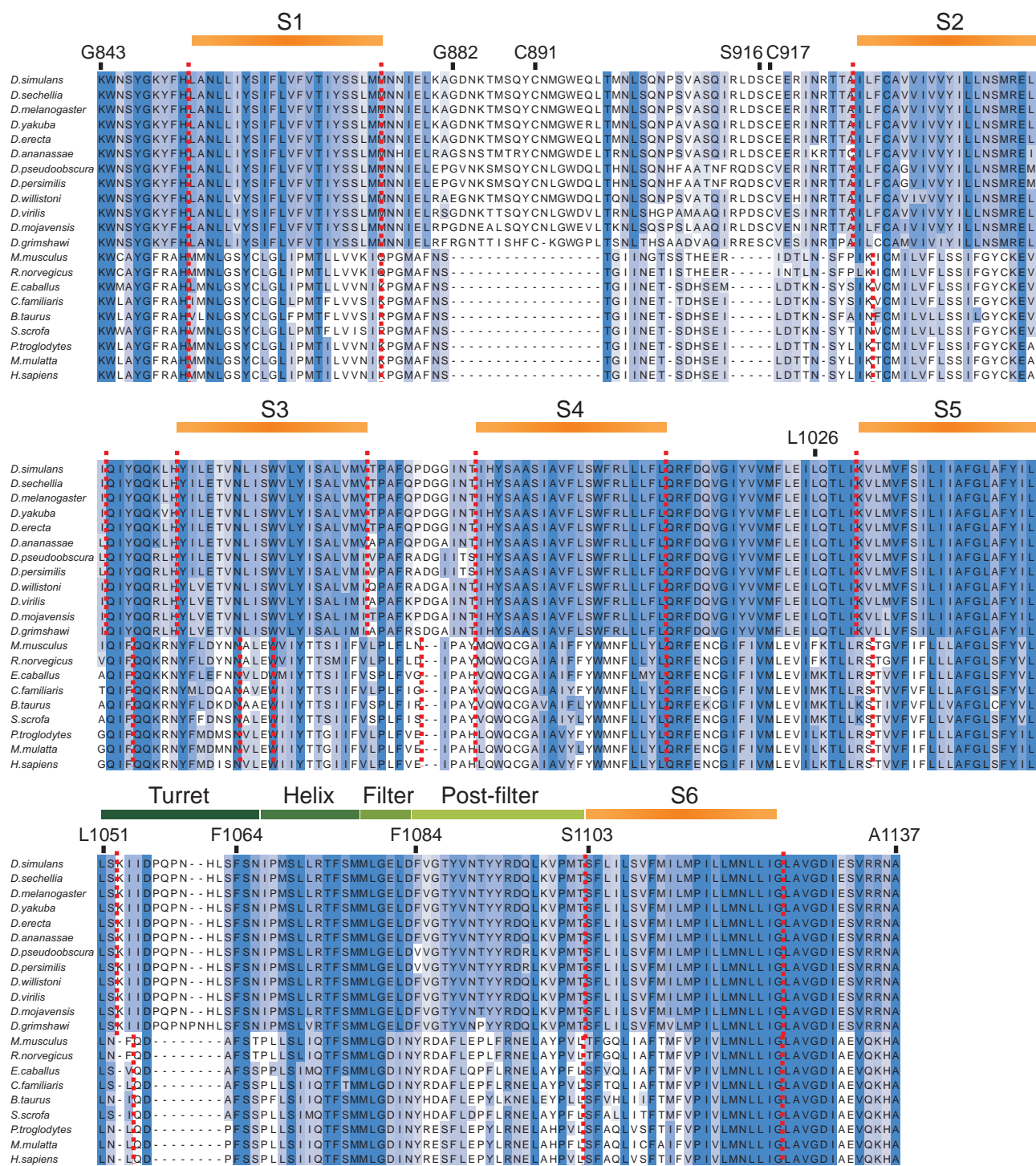
**Supplementary Figure 2.** Temperature sensitivity of hTRPA1. **(a)** hTRPA1 is not activated by heat. Currents were normalized to the peak current at +100 mV. Inset shows  $IV$  curve at  $25\text{ }^{\circ}\text{C}$  **(b)** Voltage dependent activation of hTRPA1 is shifted leftwards upon cooling (inset shows representative whole-cell current traces at  $24\text{ }^{\circ}\text{C}$ ).

**Supplementary Figure 3.** Robust expression of chimeric TRPA1 channels in *Drosophila* S2 cells



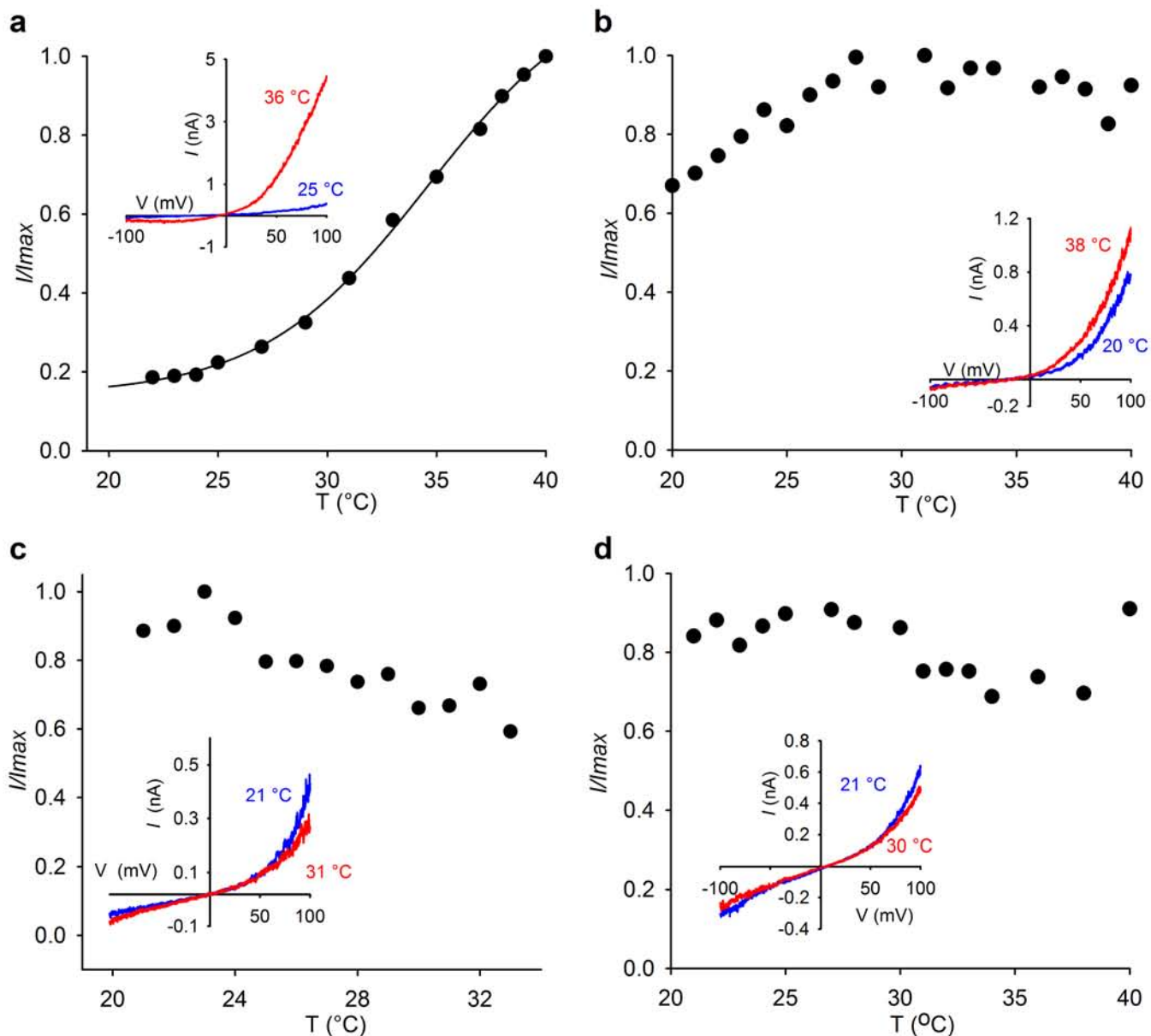
**Supplementary Figure 3.** Robust expression of chimeric TRPA1 channels in *Drosophila* S2 cells. V-5-epitope tagged chimeric channels DHH (a), DDH (b), HDH (c), HHD (d) are appropriately trafficked to the plasma membrane.

## Supplementary Figure 4. Sequence alignment of transmembrane region of *Drosophila* and mammalian TRPA channels



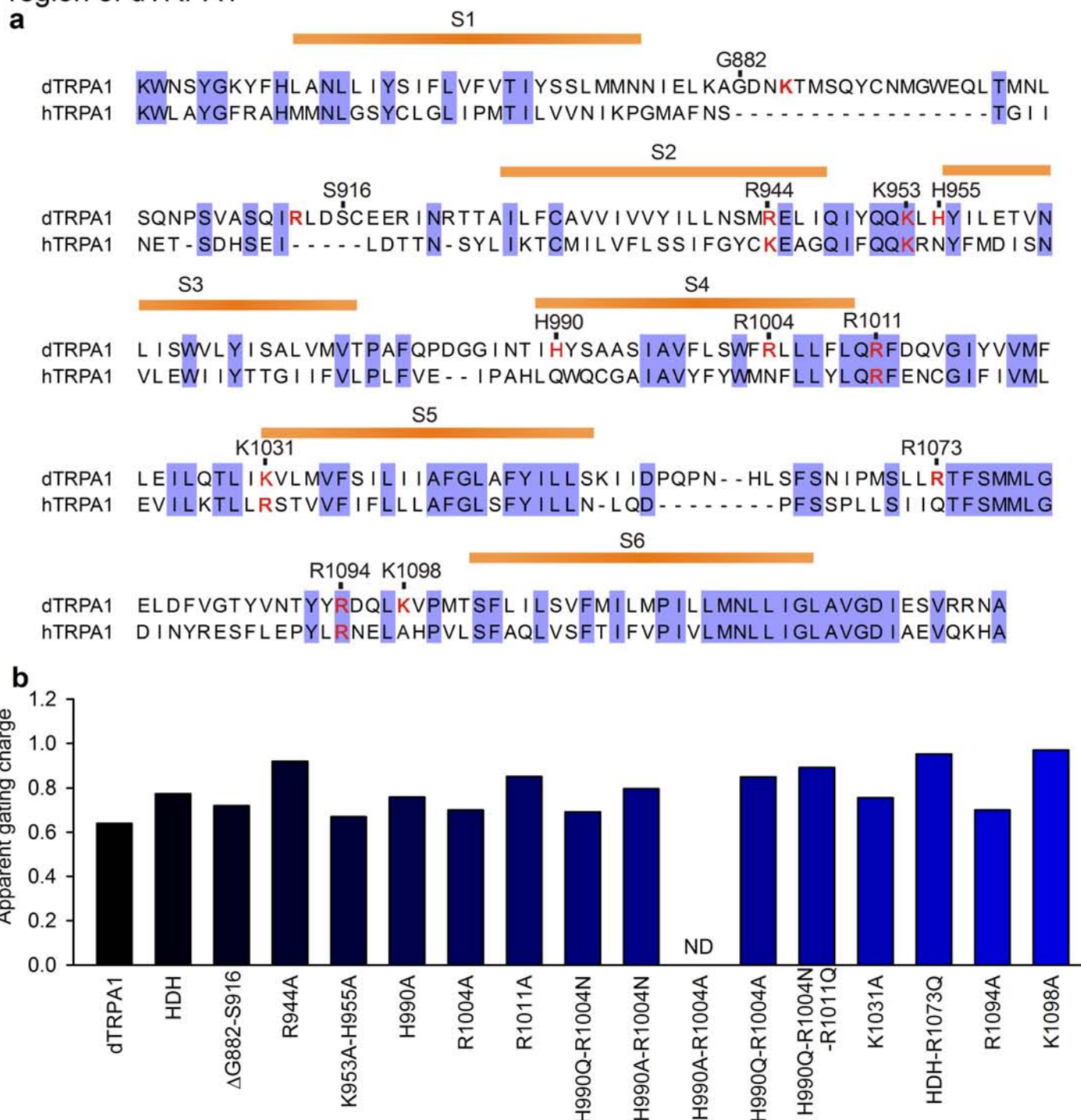
**Supplementary Figure 4.** Sequence alignment of transmembrane region of *Drosophila* and mammalian TRPA channels. Multiple sequence alignment of the transmembrane region of *Drosophila* and mammalian TRPA channels generated using ClustalW2. Predicted membrane spanning regions and putative structural elements in the pore are highlighted. Marked residues indicate junction points or point mutations referred to in the text. Amino acid numbers are derived from Uniprot entries Q7Z020, TRPA1\_DROME and O75762, TRPA1\_HUMAN.

## Supplementary Figure 5. Temperature sensitivity of mutant dTRPA1 channels



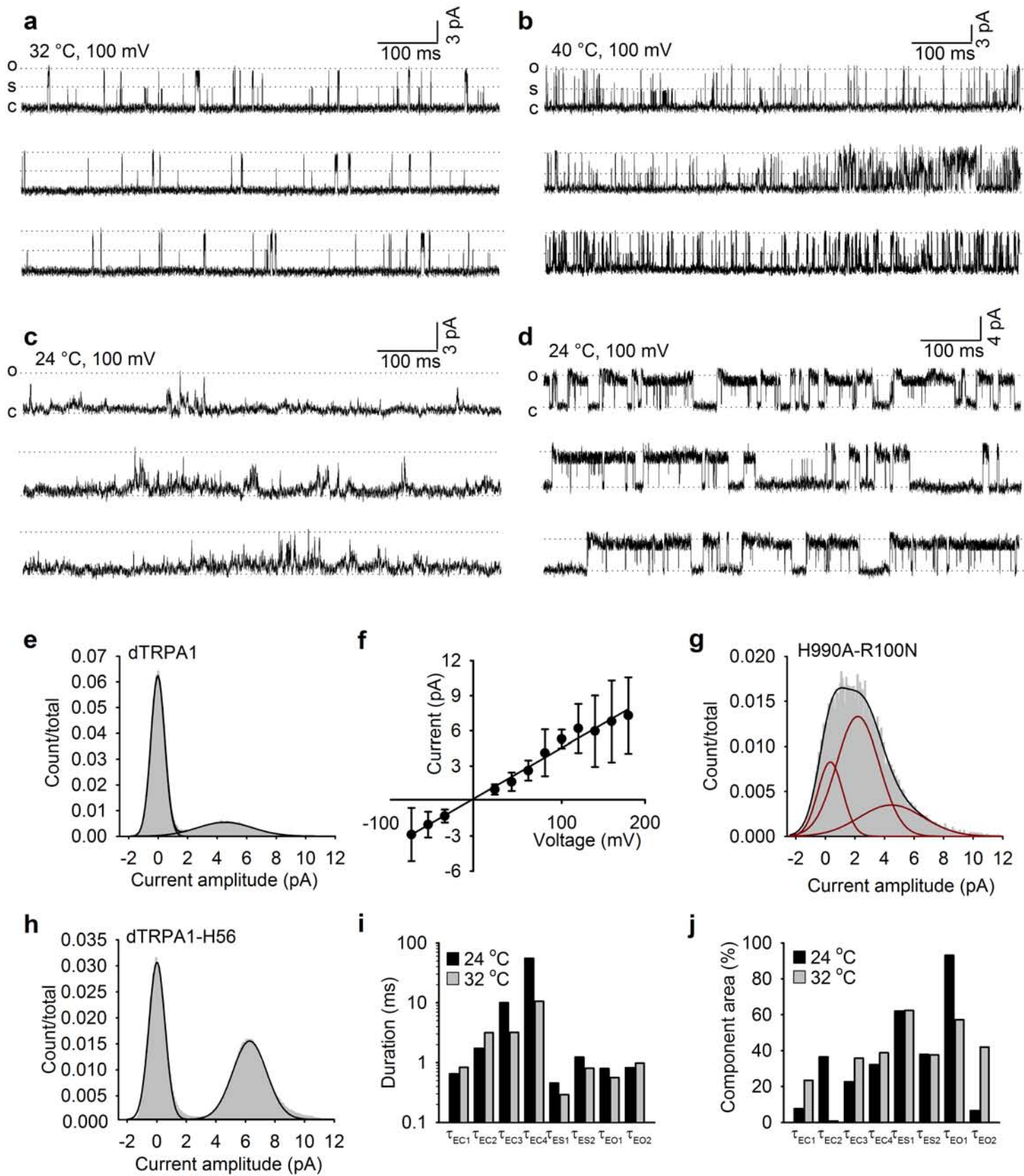
**Supplementary Figure 5.** Temperature sensitivity of mutant dTRPA1 channels. **(a)** Mutation of both extracellular Cysteine residues to Serines (C891S + C917S) between S1 and S2 does not effect temperature sensitivity of dTRPA1. **(b)** The M1111T mutation in S6 reduced heat sensitivity. **(c)** The N1066+I1067 to S mutation in the pore helix reduced heat sensitivity. **(d)** The R1073K in the pore helix abolished heat sensitivity. Currents were normalized to the peak current at +100 mV and solid lines are best fits to Boltzmann functions. Insets show representative  $IV$  curves.

**Supplementary Figure 6.** Neutralization of charged residues in the transmembrane region of dTRPA1



**Supplementary Figure 6.** Neutralization of charged residues in the transmembrane region of dTRPA1. **(a)** Sequence alignment of the transmembrane region of dTRPA1 and hTRPA1 showing mutagenesis strategy to neutralize charged amino acids. Numbered residues indicate the mutagenesis point, red lettering indicates the positively charged amino acids that were neutralized. Two positive residues were removed by the ΔG882-S917 deletion, K953 and H955 in S3 were neutralized together, and H990, R1004 and R1011 in S4 were mutated singularly, doubly or together. In the pore region R1073 was mutated in the HDH chimera and R1094 and K1098 were neutralized in dTRPA1. **(b)** Apparent gating charge for the indicated charge neutralizing mutations. H990A-R1004A was not functional and  $Z_{app}$  could not be determined.

## Supplementary Figure 7. Single channel analysis of dTRPA1 and chimeric channels

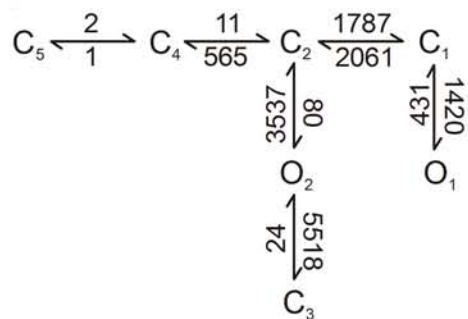


**Supplementary Figure 7. Single channel analysis of dTRPA1 and mutant channels.** Representative single channel traces of dTRPA1 mutants H990A-R1004N (**a** and **b**), R1073Q (**c**) and dTRPA1-56H (**d**). Open, subconductance and closed states are indicated with dotted lines. (**e**) Single channel I-V curve of dTRPA1 at 32 °C. (**f – h**) Amplitude histograms fitted with Gaussian functions at 100 mV and 25 °C of dTRPA1 (**f**), H990A-R100N (**g**) and dTRPA1-56H (**h**). (**i** and **j**) Time constants (**i**) and areas (**j**) of exponential components of closed (EC1-EC5) and open (EO1-EO2) distributions of H990A-R100N at 34 °C and 40 °C.

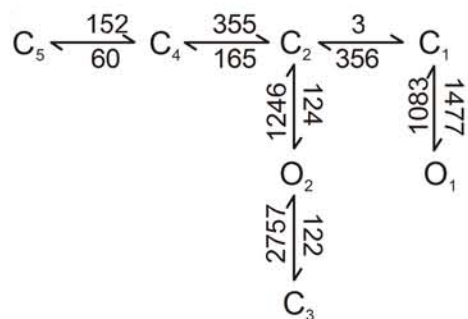
**Supplementary Figure 8.** Simulated single channel activity

a

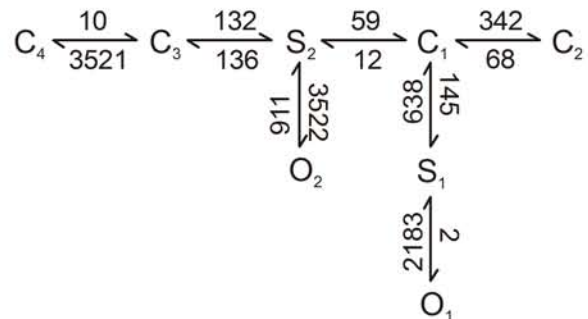
dTRPA1  
20°C



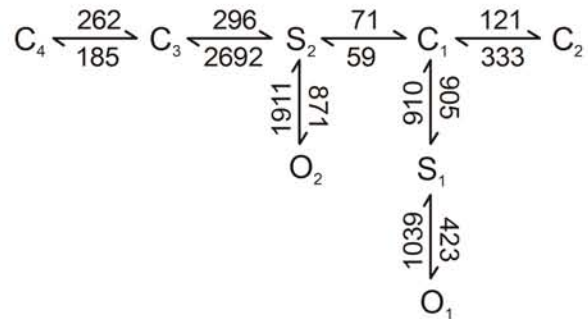
40°C



H990A-R1004N  
20°C

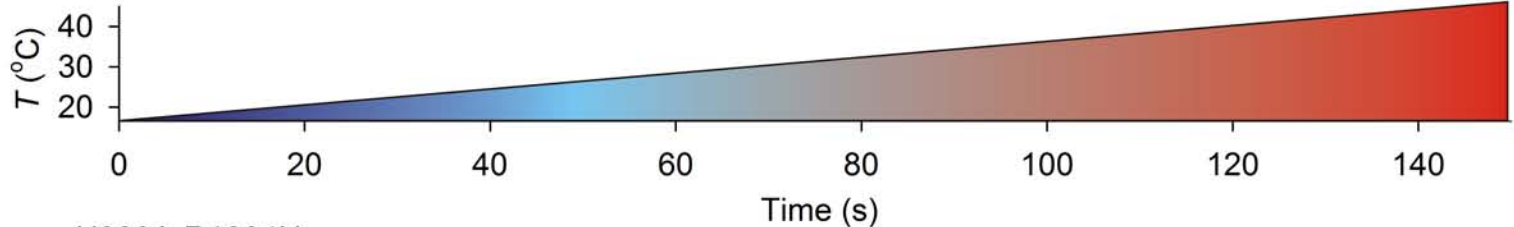


40°C



b

## dTRPA1

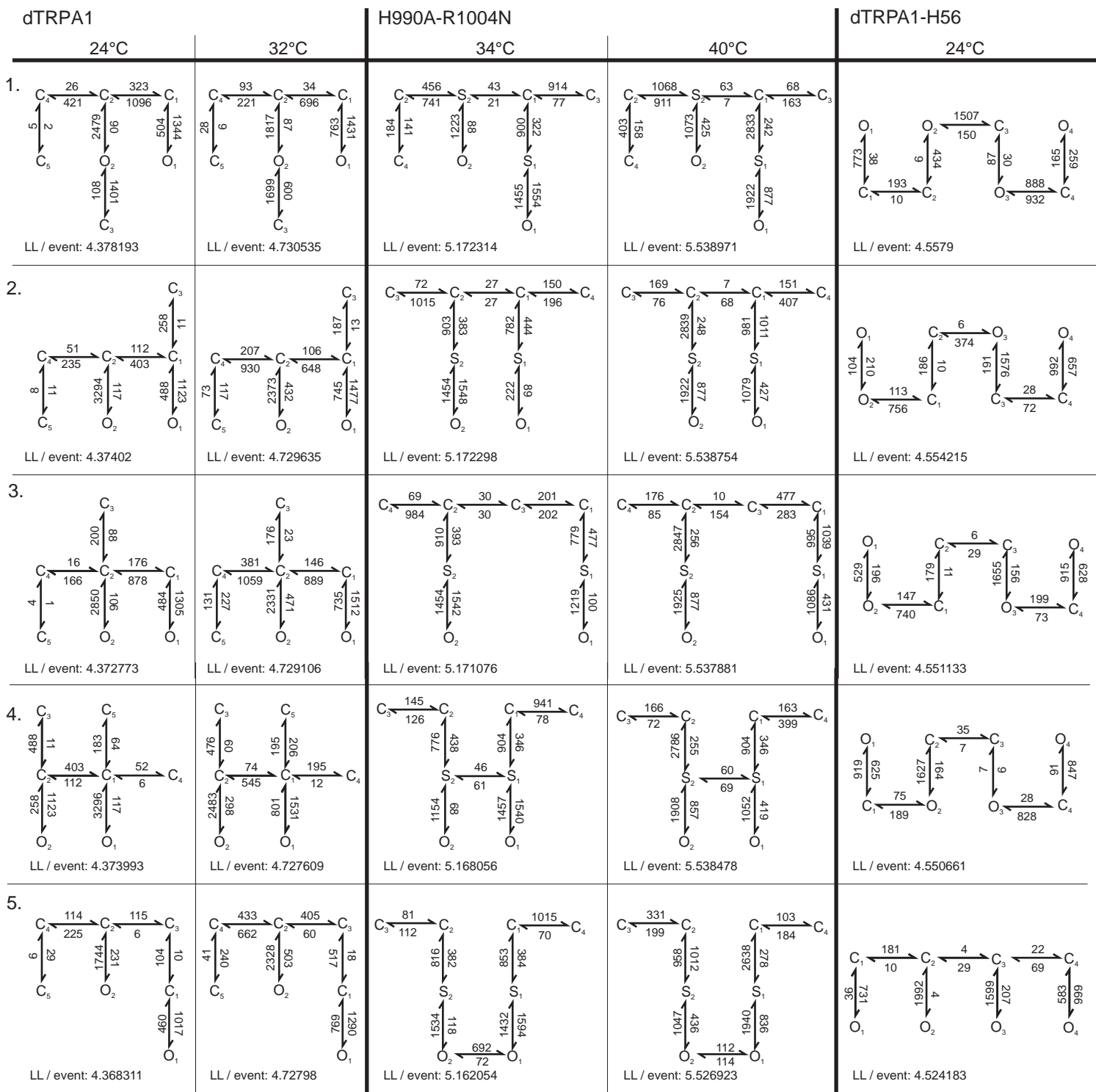


H990A-R1004N



**Supplementary Figure 8.** Simulated single channel activity of dTRPA1 and H990A-R1004N. (a) Temperature dependent rate constants at 20 °C and 40 °C estimated from a global model of dTRPA1 and H990A-R100N activity. (b) Simulated single channel currents of dTRPA1 and H990A-R1004N in response to a temperature ramp from 15 °C to 45 °C.

**Supplementary Table 1.** Highest ranked schemes for dTRPA1 and mutant channels



**Supplementary Table 1.** Highest ranked schemes for dTRPA1 and mutant channels. Kinetic models for dTRPA1, H990A-R1004N and dTRPA1-H56 with the associated log-likelihood value. Rates are in s<sup>-1</sup>